Luminescence properties of tungstates and molybdates phosphors: Illustration on ALn(MO4)2 compounds (A = alikaline cation, Ln = lanthanides, M = W, Mo)

Benoit Glorieux, Veronique Jubera, Arnaud Apheceixborde, Alain Garcia

Luminescence properties of tungstates and molybdates phosphors : illustration on $ALn(MO_4)_2$ compounds (A = alkaline cation, Ln = lanthanides, M = W, Mo)

Glorieux B., Jubera V., Apheceixborde A., Garcia A.

Abtract : The photoluminescence characteristics of compounds $ALn(MO_4)_2$, with A = Li, Na, K; Ln = Y, La, Gd, Lu, M = Mo, W, are analyzed as a function of their structure. The influences of cation size and electronegativity are discussed in relation with the Struck and Fonger theory, with a view to developing one or more of those compounds as phosphors in relation with the development of white LEDs. It appears that there are various excited states implied in the absorption process, with partially radiative transfer between them. All the radiative mechanisms are strongly related to temperature. Due to their electronegativity, tungstate compounds are the most promising, compared to molybdate ones, especially those in the monoclinic $P_{2/n}$ structure.

1. Introduction :

Growing interest has emerged worldwide in the last 10 years regarding research on solid-state lighting with light emitting diodes (LED) [1], [2] and [3]. International [4], European [5] and National [6] decisions have prompted the industrial and scientific communities to develop new materials and devices for sustainable lighting, aiming to reach higher performances than incandescent and fluorescent lights in energy savings and the reduction of green house gas emissions [7].

Currently, the white light produced by a LED is obtained by combining a blue chip and a yellow one emitting phosphors: $YAG:Ce^{3+}$ [8]. But the intensity of the phosphor is much lower than that of the blue emission coming out the chip, which induces a bluish light unsuitable for daily lighting. Other approaches are used to produce a white light. Even if the phosphor-based process is the most promising, other ideas – like modifying the diode with quantum dots – are taken into consideration [9]. Organic LEDs (OLEDs) are also involved in the development of new lighting. If LEDs are more dedicated to point light source, OLEDs are suitable for larger areas, diffuse lighting and biolabelling. The main advantages of OLEDs lie in their cost, their adjustable versatility and the lack of electromagnetic field involved (compared to fluo-compact lamps) but they reach their limits in thermal and chemical stability, which has an impact on their long term performances [10].

Tungstate and molybdate compounds have been extensively studied for solid-state lighting with LED. In most cases, these structures are luminescent ion hosts in order to obtain a well defined emission property [11], [12] and [13], and more significantly to obtain intense red phosphors [14]. In these studies, the red component is analyzed in order to be added to other phosphors (green and blue) to obtain a white light by combining those three colors with a U.V. diode. This approach has to be compared with the fluo-compact discharge plasma process which uses three phosphors emitting the three primary colors due to a U.V. excitation developed in the discharge plasma in an Hg based atmosphere: Blue: $(Ba, Sr)MgAl_{10}O_{17}:Eu^{2+}$, Green: $LaPO_4:Ce^{3+}Tb^{3+}$, Red: $Y_2O_3:Eu^{3+}$ [15].

The present study aims to analyze the intrinsic characteristics of the structure in order to produce a white light without adding a luminescent ion. For that purpose, it is necessary to analyze how the anionic groups of the compound absorb and emit. This study is performed on $ALn(MO_4)_2$ compounds with A = Li, Na, K; Ln = Y, La, Gd, Lu and M = Mo, W.

To predict the efficiency of luminescence, we consider the ratio between the probabilities of radiative and non-radiative transitions of a luminescent centre. For this purpose, the one-configurational coordinate diagram can be used as a first approach. Thirty years ago, G. Blasse discussed the influence of the three main variables introduced in this model [16].C. W. Struck and W. H. Fonger introduced this Single Configurational Coordinate model (SCC) but they treated it quantum mechanically (QMSCC) [17], [18]. Within those models, the key parameters necessary to estimate relatively the efficiency are:

- ΔR: dimensionless Franck Condon offset parameter relating to the stretching of the chemical bonding after the absorption of excitation energy,
- ΔE: the energy difference between the minima of the excited and ground states,
- $\hbar\omega_u$ and $\hbar\omega_v$: the vibrational frequencies of the ground and excited states respectively, inside the parabola. (θ: Manneback angle with $tg^4\theta = k_v/k_u$; $tg^2\theta = \hbar\omega_v/\hbar\omega_u$; k: force constant of the parabola representing the energy level),
- I: the crossing point between the ground state and the excited state parabolas,
- ΔE': the energy difference between I point and the minimum of the excited state parabola.

The intrinsic luminescence of tungstate and molybdate compounds was observed by G. Blasse et al. thirty years ago[19], [20]. In the $CaWO_4$ scheelite-type compound, the W cation is surrounded by four oxygen atoms in a regular tetrahedral environment. We consider a one-electron charge transfer process from the oxygen 2p orbital to the 4d and 5d (Mo and W, respectively) of the M^{6+} cation. For the tungsten compounds, the ground state corresponds to the $^1A_1$ level (4d/5d°−M^{6+} (M = W, Mo)/2p^6−O^{2-} state) and the lowest energy excited state is results from the splitting of the $^3T_1$ level (4d/5 d^1−M^{5+}/2p^5−O^- state). The absorption band will be named charge transfer excitation band (EX-CTB) in the present paper. After the relaxation processes through the different vibrational levels of the excited state, electrons reach the more stable state of the lowest energy excited state (LEES) from which the system can emit photons. As the emission comes from a level associated to an electron transfer mechanism, it can be described as charge transfer emission band (EM-CTB). The energy difference between the maximum of the emission and excitation band related to the same two levels is called Stokes Shift. This value gives information about the non-radiative contribution to the relaxation processes.

The respective influence of tungstate and molybdate atoms has been discussed in the literature [21], [22] where it is evidenced that, due to the difference of Pauling's electronegativity between molybdenum and tungsten atoms and by considering a same structure, the excited states of tungstate groups are located at higher energy. The thermal quenching threshold of molybdate compounds is then reached for lower temperature.

Campos et al. [23] explain experimentally and theoretically the phenomena responsible for luminescence in $CaMO_4$ (M = W, Mo). The blue-green emission comes from the MO_4 tetrahedra slightly distorted, while the orange comes from oxygen-red due to a distortion in the long and medium range order. The influence of the oxygen vacancies is still subject to discussion.

Few publications deal with the influence of the cation (alkaline, rare earth,.) on the luminescence of M-O transitions. Z. Wang [13] and Cavalli [24] used various alkaline cations in order to distort the structure, which broadens the excitation band and enhance the absorption properties. But the relative influence of the alkaline cations on the emission phenomena has not been established yet.

2. Experimental

The reactants used were: Li_2CO_3 (Strew chemicals, 99.999%), K_2CO_3 (Proanalysis, 99%), Na_2CO_3 (Roth, 99.8%), Gd_2O_3 (Philips, 99.99%), La_2O_3 (Roth, 99.99%), Lu_2O_3 (Strew chemicals, 99.999%), Y_2O_3 (Rhodia, 99.99%), WO_3 (Alfa Aesar, 99.8%) and MoO_3 (Alfa Aesar, 99.95%).

Lanthanum oxide was previously heated at 800 °C overnight, in order to remove all the hydroxide and carbonate of from the powder.

The reactants were stoichiometrically weighed, ground in an agate mortar and then thermally treated at 800 °C under oxygen atmosphere during 30 h, with a heating rate of 5 °C/min.

The x-ray patterns were obtained with a Bragg-Bentano Philips PW1820 diffractometer working with the Cu Kα radiation, thanks to a backward monochromator. The patterns were analyzed using the Eva Bruker® software and compared to the PDF database using the FindIt ICSD software. The spectra were smoothed using a reverse FFT routine and the peaks were identified by a second derivative technique. The cell parameters were calculated using Rietveld refinement with the FullProf software [25].

Luminescence properties were analyzed using a spectrofluorimeter SPEX FL212. Excitation spectra were corrected for the variation of the incident flux as well as emission spectra for the transmission of the monochromator and the response of the photomultiplier. This equipment is composed of a 450 W xenon lamp, an excitation double monochromator, a sample holder, an emission double monochromator and a photomultiplier tube.

This equipment was used to perform a zero order total excitation analysis which implied setting the emission monochromator in a mirror position (Zero order) to allow the photomultiplier tubes to collect all the luminescence emission for a scanned excitation wavelength. This technique was used to discriminate between the various EX-CTB and to analyze energy transfer between them, in contrast with regular excitation spectra for a specific emission wavelength.

This equipment was also used to perform low temperature measurements, using a specific sample holder surrounded by a liquid nitrogen cryostat, in order to maintain the sample at a specific temperature between 80 K and room temperature.

3. Results and discussion

3.1. Structural determination

Table 1 refers to the structural determination of each synthesized compound.The peaks sizes and shapes are similar for all the XRD spectra, meaning that all the compounds get similar particle size and crystallization degree. This point was confirmed by SEM experiments.

The measured cell parameters are in agreement with literature data. Their evolutions are quite logical: within a same structure; cell parameters are directly proportional to the cation size. Knowing that the size of rare earth elements and alkaline cations decreases in the following order: La > Gd > Y > Lu and K > Na > Li, cell parameters will follow the same evolution. Because Mo^{6+} and W^{6+} radii are similar (0.59 Å and 0.60 Å respectively), no clear influence of the tungstate and molybdate cations is observable on the cell parameters for compounds containing identical rare earth elements and alkaline cations.

The optical properties of these compounds were analyzed as a function of their structure. All the photoluminescence experiments were performed and recorded within the same configuration and experimental conditions (slits aperture, gain), so that all the intensities are comparable.

3.2. Monoclinic $P_{2/n}$ (S.G. 13)

This structure refers to $LiLu(WO_4)_2$ and $LiY(WO_4)_2$ compounds. In this structure [26], the tungsten cation is surrounded by six oxygen neighbors in an octahedral site. Each octahedron is linked to the next one by a common edge to make isolated $[WO_4]_n$ monodimensional chains.

Photoluminescent experiments were performed at room and low temperature. Results shown correspond to the room temperature spectra and the emission intensity as a function of the temperature (Fig. 1).

For both compounds; the maxima of the excitation and emission bands are located at about 280 nm and 500 nm, respectively. The full width at half maximum (FWHM) of the emission band is about 5950 cm^{-1}.

The intensity of the lutetium-based compound is slightly more intense. The maxima of the excitation and emission spectra are shifted to the higher energies in comparison with the yttrium-based compound. The Stokes shift values are quite similar, about 15,850 cm^{-1} for both compounds.

Low temperature measurements were performed on the lutetium compound. Decreasing temperature did not reveal any relevant non previously observed phenomena. The maximum of the emission band remains the same, while a slight narrowing of the excitation and emission bands is obtained when temperature decreases. This modification of the FWHM is related to the reduction of the thermal population of the vibrational levels as the temperature decreases. At 100 K, the intensity observed is five times higher than the one recorded at room temperature. This thermal quenching is directly related to the Franck Condon parameter value and to the low position of the LEES, which allows a direct relaxation via the I point to the ground state. The Stokes Shift is not modified whatever the temperature applied for these measurements.

As no modification of the emission spectra was observed for different excitation wavelengths, one can suggest that the radiative emission comes from the LEES.

In order to confirm this hypothesis, zero order experiments were performed. In this configuration, the emission monochromator was used as a mirror. There were no emission wavelength monochromator selection, meaning hence all the radiations are recorded for a scanned excitation wavelength. A 351 nm filter was positioned after the sample in order to remove all the reflected photons and to collect only emission light.

It appears (Fig. 1) that the regular excitation spectrum recorded for λ_{em} equal to 500 nm is almost equivalent to the zero order excitation spectrum. Only a slight narrowing of the band is revealed. This confirms that the excitation energy is relaxed through the different excited states until it reaches the lowest energy state from which radiative emission can be observed.

3.3. Tetragonal I41/a (88)

This structure refers to $LiLn(WO_4)_2$ (Ln = Gd, La), $LiLn(MoO_4)_2$ (Ln = Lu, Y, Gd, La), $NaLn(MO_4)_2$ (Ln = Lu, Y, Gd, La; M = W, Mo), $KLa(MO_4)_2$ (M = W, Mo) [27]. In this structure, the tungsten and molybdenum cations are surrounded by four oxygen neighbors in a tetrahedral polyhedron. Each tetrahedron is isolated from the other one.

The results in Fig. 2 refer to experiments performed at the maximum excitation and emission intensity at room temperature.

The experiments performed on $LiLn(MoO_4)_2$ compounds did not reveal any significant luminescence intensity. This point was already noted by Zaushitsyn et al. [31]. It seems that the thermal quenching threshold is rapidly reached with the increase of the temperature, and that the room temperature intensity is already strongly affected by this phenomenon. No additional investigations were performed on these compounds.

The related Stokes Shifts are reported in Table 2.

For all the other samples, the photoluminescence emission is composed of a broad band, starting between 350 and 400 nm, and ending at a high wavelength (higher than 700 nm).

The comparison of results on tungstate and molybdate compounds containing the same alkaline and rare earth cations shows that the tungstates luminescence is more intense, and that their maximum of emission is located at higher energy. As mentioned in the introduction, the phenomenon has already been discussed in various publications [21], [22], and is due to the difference in Pauling's electronegativity.

The electron transfer from oxygen to the molybdenum cation is easier than the charge transfer to the tungsten cation because of a higher electronegativity of molybdenum. This implies a lower position of the molybdenum CTS. The lower corresponding value of ΔE' induces a higher probability of non-radiative de-excitation via the I crossing point. For a same alkaline cation, the thermal quenching effect is higher in molybdenum compounds than in tungsten compounds.

For the Li-based compounds, the luminescence intensity decreases when the size of the rare earth element increases. In the same time, a red shift of the emission appears. The Stokes Shift value increases from about 18,600 cm^{-1} to 19,750 cm^{-1} for the gadolinium and lanthanum matrices, respectively. Contrary to the other tungstates, a higher Stokes Shift, for almost the same energy position of the LEES, is caused by a greater ΔR and a smaller ΔE'. The result is a lowering of the temperature threshold and a lower efficiency at room temperature.

This tendency is less marked for the monoclinic $P_{2/n}$ compounds. In this case, the limiting factors are both ΔR and ΔE' parameters.

In the case of the Na-based samples, the tendency is the opposite. By substituting the rare earth element, from yttrium to lanthanum, a global blue shift of the excitation and emission spectra is observed. This is associated with an increase of the global emission and is in agreement with Kato et al. results [32]. The global intensity of the sodium-contained compounds is higher than that of the lithium-contained ones. This point might be due to the difference in size between the alkaline and the rare earth elements. In an eight coordination polyhedron, ionic radii are: $r_{Li+} = 0.92Å < r_{Lu3+} = 0.977Å < r_{Y3+} = 1.019Å < r_{Gd3+} = 1.05Å < r_{La3+} = 1.16Å < r_{Na+} = 1.18Å$. Both alkaline and rare earth cations occupy randomly the same crystallographic site. The closer the size of the alkaline, compared to the rare earth ions, the higher the intensity observed.

These phenomena could/may be linked to the rigidity of the structure. While having a distorted structure due to high difference in size, the re-arrangement of the chemical bonding after absorption of the excitation beam impacts the ΔR parameter. This leads to an increase of the Stokes shift value which gives rise to a decrease of the luminescence if the position of the LEES is the same. But due to the observed blue shift in the Na-based compounds, these levels are at higher energy. It seems that in this case the ΔE' parameter is predominant over the ΔR value, hence luminescence intensity increases with rare earth radii.

Another parameter can be considered to compare the global intensity variation between the lithium and the sodium compounds: the $\hbar\omega_v$ parameter (phonon energy). As the sodium weight is greater, one can imagine that this value is

smaller for the sodium-contained compound. Then a lower vibrational frequency would lead to a higher thermal quenching threshold. This argument on the variation of phonon energy is valid if all the other parameters remain unchanged. But in the present situation, the positions of LEES in Na-based compounds being at higher energy (excitation Band at lower wavelength), the resulting greater ΔE' value is in fact the determining factor for the less pronounced thermal quenching.

Low temperature spectra were performed on selected compounds (Fig. 3), in order to analyze more precisely the luminescence phenomena and to distinguish the various processes leading to radiative de-excitation.

Two cases can be distinguished:

* $LiGd(WO_4)_2$, $NaGd(WO_4)_2$, and $NaGd(MoO_4)_2$, get similar shapes whatever the temperature. Only a broad absorption band is visible,

* $NaY(MoO_4)_2$ and $NaLa(MoO_4)_2$ present a narrow band at about 320 nm followed by a broad shoulder at higher energy. Only the $NaLa(MoO_4)_2$ is represented in the Fig. 3.

In the first case, by considering the non-symmetric shape of the band, various EX-CTB are detected in the excitation range. But as for $LiLu(WO_4)_2$ and $LiY(WO_4)_2$ compounds previously mentioned, only one gaussian curve is necessary to fit the emission spectrum data, which means that the emission comes only from the LEES. No significant variation of the Stokes shift value is observed. The broader shape of the excitation and emission bands of the lithium-contained compounds may indicate a higher reorganisation of the chemical bonding after absorption of the excitation energy.

For $NaY(MoO_4)_2$ and $NaLa(MoO_4)_2$ samples, the different spectra reveal clearly the existence of two kinds of luminescence. The excitation spectra are composed of two bands: a broad and less intense one below 300 nm and a narrow and intense band peaking at 320 nm. Exciting at about 280–290 nm leads to an emission at 600 nm, while exciting at 320 nm implies an emission at 660–670 nm. A slight blue shift of the absorption bands and a decrease of the Stokes shift are caused by decreasing the temperature.

In order to better understand the differences of optical characteristics between those tetragonal samples, zero order excitation experiments were performed and compared to regular room temperature excitation experiments. Results are shown in Fig. 4.

From a zero order excitation the spectral distribution of the excitation bands was different from that coming from a defined emission wavelength. In all cases, the zero order experiments revealed two absorption ranges: a broad band at 240–260 nm and a narrower band at lower energy. More selective excitations were then performed to obtain the corresponding emission band. Generally excitations at high energy lead to emission peaking at high energy and excitation in the LEES induce another emission at low energy. From these experiments we can observe different excited states and conclude that there is no complete transfer between them.

This behavior differs completely from that of the monoclinic sample $LiLu(WO_4)_2$. For the tetragonal compounds, different EM-CTB have been reported. Excitation spectra have revealed transfer phenomena. Depending on the alkaline/rare earth pairs, energy transfer between these excited states is more or less efficient.

3.4. Monoclinic $C_{2/c}$ (S.G. 15)

This structure refers to $KLn(WO_4)_2$, with Ln = Lu, Y and Gd. In this family [28], the tungsten cation is surrounded by six oxygen neighbors in an octahedral shape. Each octahedron is linked to three other octahedra by sharing edge and corner to form double chains.

The photoluminescence experiments are reported in Fig. 5.

A weak luminescence for gadolinium and yttrium-based compounds can be detected, while the lutetium compound is twenty times more intense. One can observe a narrowing of the bands and a shift to higher energy. The calculated Stokes Shift are equal to 11,865 cm^{-1}, 13,090 cm^{-1} and 14,558 cm^{-1}, for the lutetium, yttrium and gadolinium compounds respectively. Compared to all the other compounds previously treated, the Stokes Shift are among the smallest and therefore the excitation bands are narrow. One can suggest that the higher connection between anionic polyhedra improves the structure rigidity, leading to less dispersed positions of the EX-CTB.

Compared to the other monoclinic structure $P_{2/n}$ (13), and by considering the lower value of the Stokes shift, one would have expected a higher luminescence efficiency which is clearly not the case. As noted by Totardi et al. [33] in their communication about the $ALn(WO_4)_2$ (A: alkaline cation, Ln: rare earth element) luminescence, the $AY(WO_4)_2$ matrices

possess two different types of W-O distances, short and long ones, along chains constituted composed of metal coordination polyhedra. The strong connection across the chains is made by edge-sharing pairs of WO_6 octahedra. To explain the lack of efficiency of the $KY(WO_4)_2$ compared to that of $CsLu(WO_4)_2$, Totardi et al. propose the delocalization of the electronic charge in the tungstate double chain. The luminescence behavior of the K versus Li-contained monoclinic matrices is the same. One can suppose that a delocalization of the electron over the two chains reduces the radiative probability in the system.

The spectral distribution of the excitation spectra are different from the other compounds, especially at higher wavelength, which could be explained by the size of the potassium cation. Being bigger than the other alkalines, its phonon energies$\hbar\omega_u$ and $\hbar\omega_v$ are relatively weak. Moreover only one excitation band and one emission band are revealed, without modification of the Stokes Shift, this can be associated with only one excited level. One can also notice that the emission band is really broader than the excitation one in the configurational model described by Struck and Fonger [18]. This means that the shape (force constant) of the parabola of the GS and the excited state are very different with lower phonon energies in the excited state, which induces a narrow excitation band. (θ: Manneback angle < 45°; $tg^4\theta = k_{LEES}/k_{GS}$; $tg^2\theta = \hbar\omega_{LEES}/\hbar\omega_{GS}$; k: force constant of the parabola representing the energy level).

3.5. Orthorhombic Pbcn (S.G. 60), triclinic P-1 (S.G. 2)

These structures refer to $KLn(MoO_4)_2$, with Ln = Lu, Y and Gd. The lutetium and yttrium-based compounds are orthorhombic, while the gadolinium based one is triclinic. In these compounds [29], [30], the molybdenum cation is surrounded by four oxygen neighbors in a tetragonal shape isolated from the others.

The compounds related to this structure didn't reveal any significant luminescence phenomena. As described in the literature [34], the lack of intensity could be attributed to thermal quenching. No further experiments were performed on these compounds which don't present interesting properties for lighting application.

3.6. Comparison of compounds

On the one hand, one can observe that all the luminescence of molybdenum matrices is strongly affected by temperature. No significant intensity variation can be noticed. This results mainly from the too low energy position of the Mo-O LEES (ΔE parameter) that allows a direct non-radiative relaxation through the different vibrational levels to the ground state. This parameter is related to the Pauling's electronegativity of molybdenum compared to that of tungsten.

On the other hand, nearly all the tungsten matrices show radiative emission at room temperature.

Results of all the photoluminescence experiments were compared by integrating the area of the emission bands at room temperature. Results are shown in Fig. 6.

Fig. 6 illustrates that the size difference between the alkaline cation and the rare earth element has to be taken into account to predict the efficiency of the materials. A high size difference is linked to a local distortion of the crystallographic array what finally impacts the O-W chemical bonding in the metal coordination polyhedron. A large value of ΔR parameter facilitates the thermal quenching processes. On the opposite, this value is limited for matrices in which the difference between alkaline/rare earth element radii sizes is reduced, leading to an increase of the luminescence efficiency.

3.7. Chromatic coordinates

The chromatic coordinates of all the samples having intense luminescence characteristics at room temperature were calculated, using the CIE model [35]. Those measurements were performed on the maximum of luminescence intensity. Results are shown in Fig. 7.

Calculations of trichromatic coordinates of matrices which present luminescence at room temperature are almost all located in the white part of the diagram. The results range from blue (0.17, 0.22) to yellow (0.42, 0.46), passing by the green region, and over the white zone (0.33, 0.33). The (x,y) coordinates seem to summarize the earlier discussion about the luminescence intensities. The molybdate compounds appear clearly yellower than the tungstate compounds, which is due to their difference in Pauling's electronegativity and to the red shift of the emission spectra.

By comparing the chromatic coordinates as a function of the alkaline cations, the potassium induces a blue color. For tetragonal compounds, the greater the difference of cation size between alkaline and rare earth, the yellower the chromatic coordinates.

4. Conclusion

An extensive study of luminescence characteristics of $ALn(MO_4)_2$ (with A = Li, Na, K; Ln = Y, La, Gd, Lu; M = Mo, W) was performed by photoluminescence at room temperature, at low temperature and in a zero order configuration. All the compounds were synthesized following an identical high temperature solid state reaction and get similar particles size and crystallization degree. The first analyses have shown one broad band for the excitation and the emission, for all samples. But deeper analyzes reveal that their characteristics can be sorted out as a function of the structure, the size of the cation and the Pauling's electronegativity. The low temperature measurements and the zero order experiments reveal various excited transfer states which give rise to partial non-radiative transfers between them. The luminescence behavior can be explained by considering the three main parameters ΔE, ΔR and $\hbar\omega$, but it is still unclear whether there is a direct relation with structural characteristics like the metal coordination polyhedra or their connection inside the crystallographic structure.

The present work is a first step before adding and modifying the compounds in order to synthesize phosphors materials dedicated to white LEDs. Adding a solid solution between molybdenum and tungsten would modify the position of the excitation and emission bands but the shift would not be sufficient to obtain an absorption range in adequacy matching the current commercialized diodes. Moreover, some of these matrices which seem to be promising (ex: $LiLu(WO_4)_2$), may be selected and modified by the introduction of a dopant. In this case, one can combine the intrinsic luminescence of the matrix with the emission of the dopant.

Acknowledgments

The authors wish to thank Dr Cédric Desplanches and Dr Corine Mathonière, ICMCB (France) for the numerous fruitful discussions on the molecular approach of charge transfer phenomena.

References

[1] D. Gacio, J. Cardesin, E.L. Corominas, J.M. Alonso, M. Dalla-Costa and A.J. Calleja, *IEEE Ind. Appl. Soc. Annu. Meet.* **1-5** (2008), pp. 83–87.

[2] S. Dalmasso, B. Damilano, C. Pernot, A. Dussaigne, D. Byrne, N. Grandjean, M. Leroux and J. Massies, *Phys. Status Solidi (a)* **192** (2002), p. 139. [3] N.C. Yeh and J.P. Chung, *Renew. Sust. Ener. Sav.* **13** (8) (2009), pp. 2175–2180.

[4] E. Heuvelink and M.M. Gonzalez-Real, *Proc. Int. Symp. High Tech. for Greenhouse Syst. Man.* **1&2** (801) (2008), pp. 63–74.

[5] V. Harle, N. Hiller, S. Kugler, B. Hahn and N. Stath, *Mat. Sci. Eng. B.* **61** (2) (1999), pp. 310–313.

[6] http://www.developpement-durable.gouv.fr/IMG/pdf/2-Convention_ampoules_cle7ec3ee.pdf.

[7] M.I. Baraton, *Int. J. Nanotech.* **6** (9) (2009), pp. 776–784.

[8] S.F. Wang, K. Koteswara Rao, Y.C. Wu, Y.R. Wang, Y.F. Hsu and C.Y. Huang, *Int. J. Appl. Ceram. Technol.* **6** (4) (2008), pp. 470–478.

[9] B. Damilano, A. Dussaigne, J. Brault, T. Huault, F. Natali, F. Demolon, P. De Mierry, S. Chenot and J. Massies, *Appl. Phys. Lett.* **90** (2008), pp. 101–117.

[10] M. Klein and K. Heuser, *Lig. Energ.* **17** (3) (2009), p. 13+.

[11] J. Wang, X. Jing, C. Yan and J. Lin, *J. Electrochem. Soc.* **152** (3) (2005), pp. G186–G188.

[12] G.H. Lee, T.H. Kim, C. Yoon and S. Kang, *J. Lumin.* **128** (2008), pp. 1922–1936.

[13] Z. Wang, H. Liang, L. Zhou, H. Wu, M. Gong and Q. Su, *Chem. Phys. Lett.* **412** (2005), pp. 313–316. [14] S. Neeraj, N. Kijima and A.K. Cheetham, *Chem. Phys. Lett.* **387** (2004), pp. 2–6.

[15] A.A. Ashryatov, *Lig. Energ.* **17** (3) (2009), pp. 34–36.

[16] G. Blasse, *J. Sol. Sta. Chem.* **27** (1979), pp. 3–8.

[17] C.W. Struck and W.H. Fonger, *J. Lumin.* **10** (1975), pp. 1–30.

[18] C.W. Struck and W.H. Fonger, *J. Chem. Phys.* **64** (1976), pp. 1784–1790.

19] G. Blasse, *Chem. Phys. Lett.* **70** (1980), pp. 1–3.

[20] C. Koepke, A.J. Wojtowicz and J. Lempicki, *J. Lumin.* **54** (1993), pp. 345–355.

[21] Z.J. Jie, A. Garcia, F. Guillen, J.P. Chaminade and C. Fouassier, *Eur. J. Solid State Inorg. Chem.* **30** (1993), pp. 773–787.

[22] M. Wiegel and G. Blasse, *Solid State Commun.* **86** (4) (1993), pp. 239–241.

[23] A.B. Campos, A.Z. Simoes, E. Longo, J.A. Varela, V.M. Longo, A.T. Figuerido, F.S. De Vicente and A.C. Hernandes, *Appl. Phys. Lett.* **91** (2007), p. 051923.

[24] E. Cavalli, P. Boutinaud, M. Bettinelli and P. Dorenbos, *J. Solid State Chem.* **181** (2008), pp. 1025–1031.

[25] T. Roisnel and J. Rodriguez-Carvajal, *Mat. Sci. Forum* **118** (2001), pp. 378–381.

[26] J.S. Kim, J.C. Lee, C.I. Cheon and H.J. Kang, *Jpn. J. Appl. Phys. Part 1, (1)* **45** (9B) (2006), pp. 7397–7400.

[27] H. Li, G. Hong and S. Yue, *Kristallografiya* **17** (1972), pp. 768–772.

[28] J. Zhang, J. Wang, K. Wang, W. Yu, H. Zhang, Z. Wang, X. Wang and M. Ba, *J. Cryst. Growth* **292** (2006), pp. 373–376.

[29] R.F. Klevtsova and S.V. Borisov, *Dokl. Akad. Nauk. SSSR.* **177** (1967), pp. 1333–1336.

[30] Y. Le Page and P. Strobel, *Acta Crystallogr. Sect. B.* **36** (1980), pp. 1919–1920.

[31] A.V. Zaushitsyn, V.V. Mikhailin, A.Y. Romanenko, E.G. Khaikina, O.M. Basovich, V.A. Morozov and B.I. Lazoryak, *Inorg. Mater.* **41** (7) (2005), pp. 766–770.

[32] A. Kato, S. Oishi, T. Shishido, M. Yamazaki and S. Iida, *J. Phys. Chem. Solids.* **66** (11) (2005), pp. 2079–2081.

[33] C.C. Totardi, C. Page, L.H. Brixner, G. Glasse and G.J. Dirksen, *J. Solid State Chem.* **69** (1987), pp. 171–178.

[34] Z.L. Wang, H.B. Liang, M.L. Gong and Q. Su, *J. Alloys. Compd.* **432** (2007), pp. 308–312.

[35] CIE, Commission Internationale de l'Eclairage Proceedings, 1931, Cambridge University Press, Cambridge (1932).

Figures :

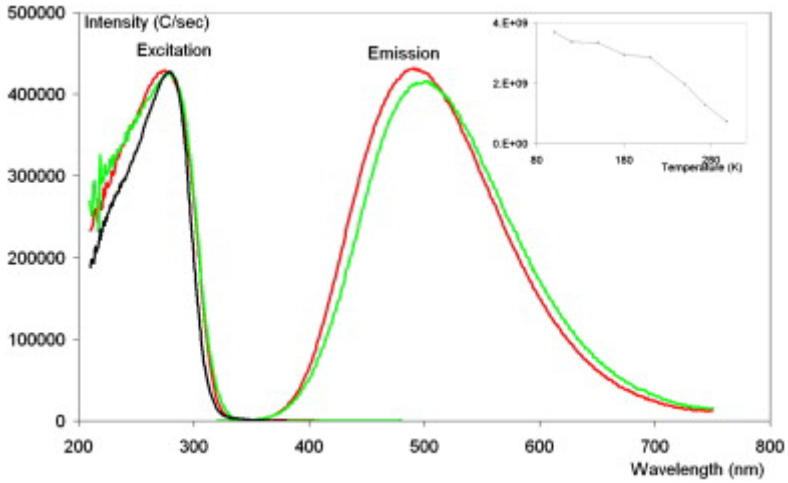

Fig. 1. Photoluminescence spectra of $LiLn(WO_4)_2$ (Ln = Lu-Red, Y-green). For excitation spectra, λ_{em} = 500 nm. For emission spectra, λ_{exc} = 280 nm. The black curve is the zero order photoluminescent excitation of $LiLu(WO_4)_2$. Inset graph represents the emission intensity (integrated area) of $LiLu(WO_4)_2$ as a function of the temperature.

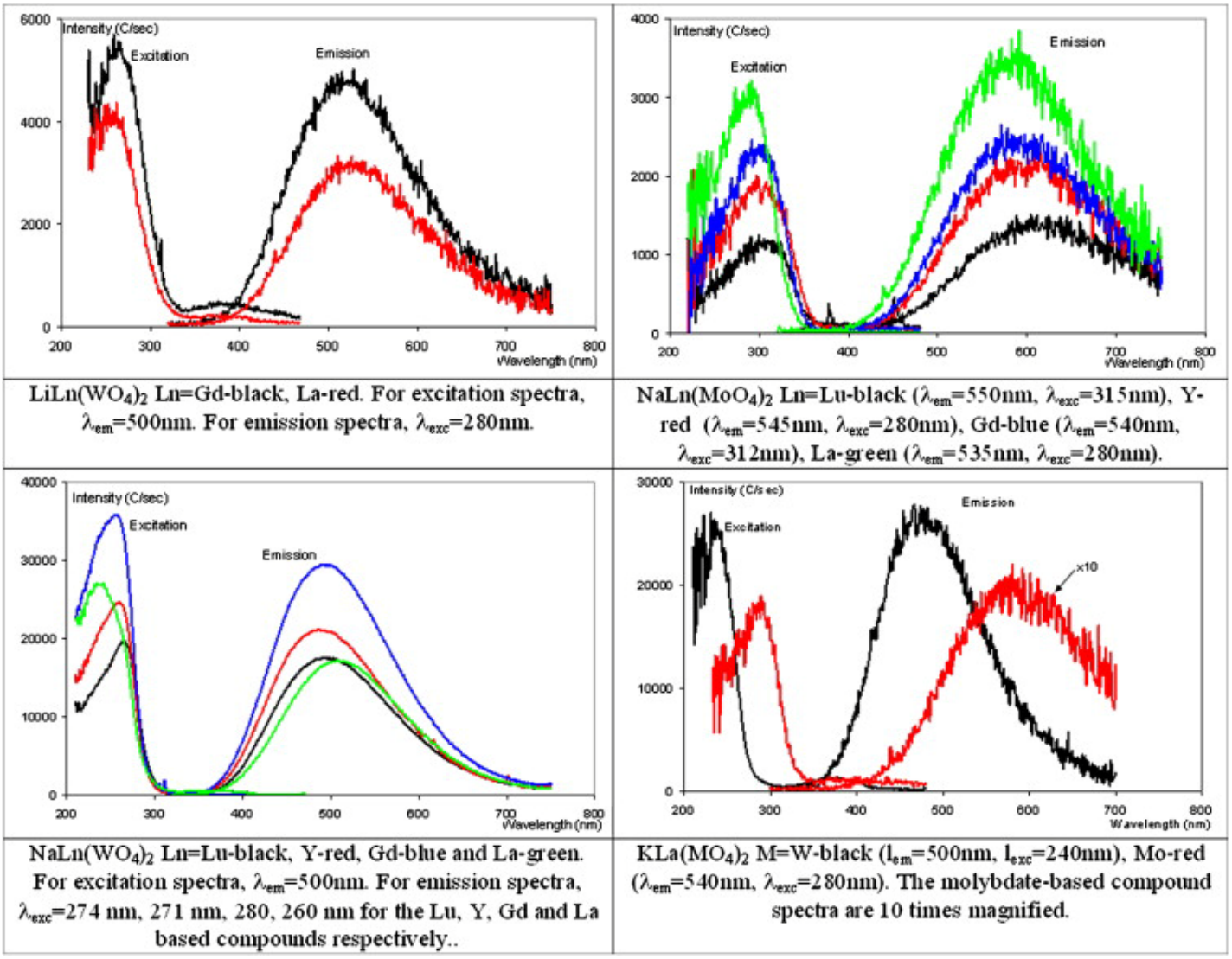

Fig. 2. Photoluminescence of tetragonal compounds.

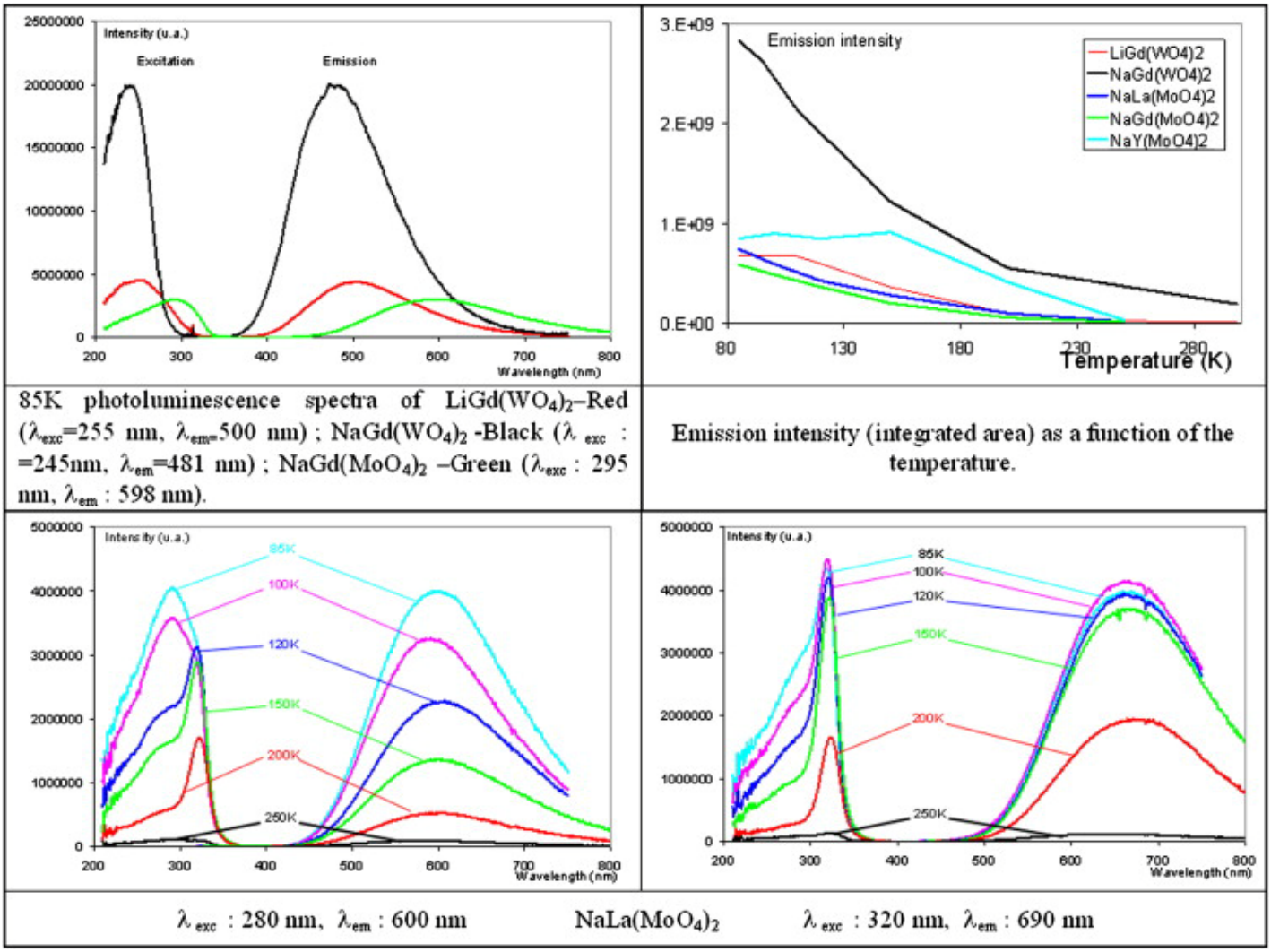

Fig. 3. Photoluminescence of tetragonal compounds versus temperature.

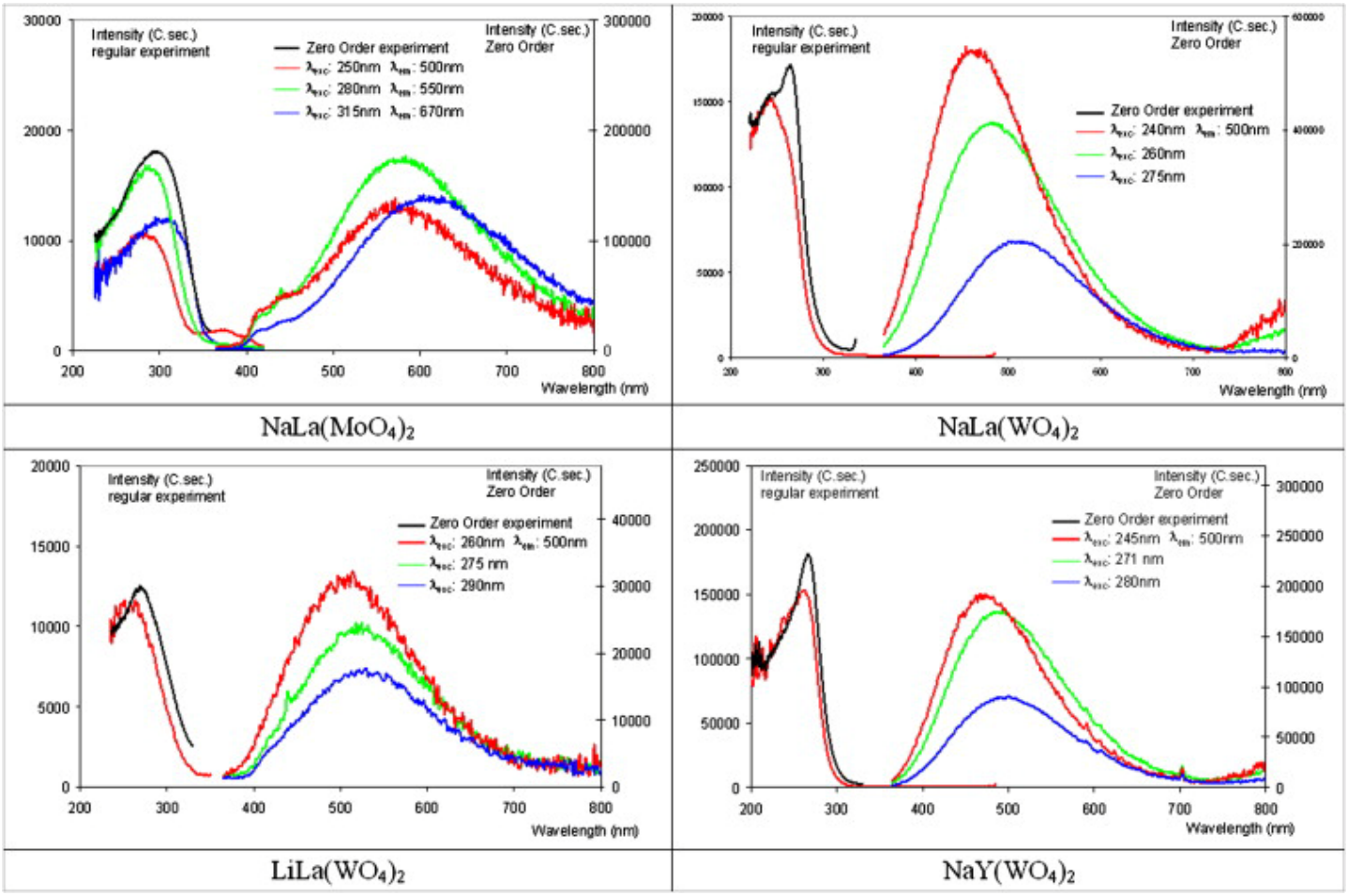

Fig. 4. Zero order photoluminescence results of tetragonal compounds.

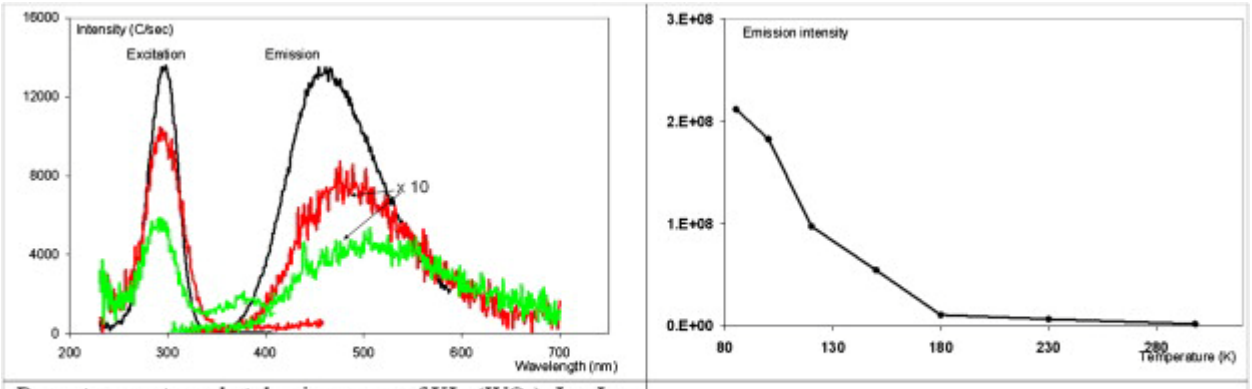

Room temperature photoluminescence of $KLn(WO_4)_2$ Ln=Lu-black (λ_{exc}=300 nm, λ_{em}=460 nm), Y-red and Gd-green ((λ_{exc}=280 nm, λ_{em}=500 nm) for two the latest compounds.

Emission intensity (integrated area) of $KGd(WO_4)_2$ as a function of the temperature.

Fig. 5. Photoluminescence of monoclinic compounds and emission intensity as a function of the temperature.

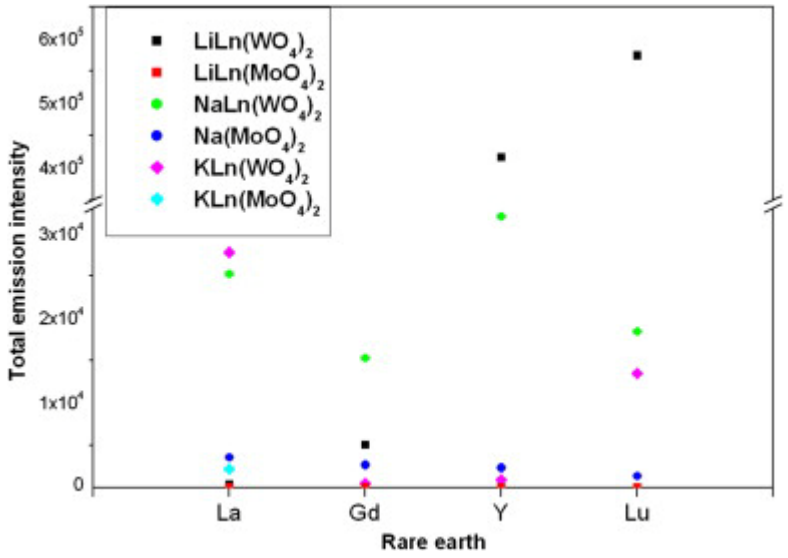

Fig. 6. Integrated intensity of the emission.

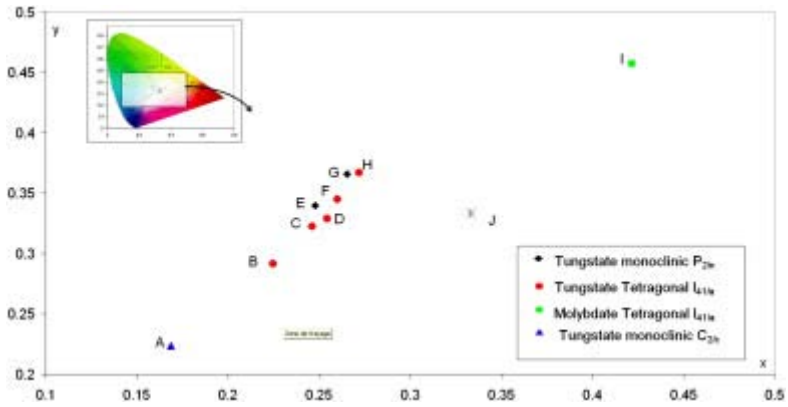

Fig. 7. Chromatic coordinates (at room temperature).A: $KLu(WO_4)_2$, B: $KLa(WO_4)_2$,C: $NaLa(WO_4)_2$, D: $NaY(WO_4)_2$, E: $LiLu(WO_4)_2$, F: $NaLu(WO_4)_2$, G: $LiY(WO_4)_2$, H: $NaGd(WO_4)_2$, I: $NaLa(MoO_4)_2$, J: white.

Tableaux :

Table 1
Structure and cell refinement.

Compounds	Structural space group (n°) and ref	Refined cell parameters			
		a	b	c	Beta
$LiLu(WO_4)_2$	Monoclinic $P_{2/n}$ (13) [26]	9.8521	5.7933	4.9861	93.1
$LiY(WO_4)_2$		9.9980	5.7985	5.0056	94.2
$LiGd(WO_4)_2$	Tetragonal $I_{41/a}$ (88) [27]	5.1968	5.1968	11.2512	90
$LiLa(WO_4)_2$		5.3237	5.3237	11.5358	90
$LiLu(MoO_4)_2$		5.1055	5.1055	11.0811	90
$LiY(MoO_4)_2$		5.1480	5.148	11.1873	90
$LiGd(MoO_4)_2$		5.1890	5.1890	11.3006	90
$LiLa(MoO_4)_2$		5.3149	5.3149	11.6630	90
$NaLu(WO_4)_2$		5.1675	5.1675	11.1886	90
$NaY(WO_4)_2$		5.2067	5.2067	11.2814	90
$NaGd(WO_4)_2$		5.2468	5.2468	11.3819	90
$NaLa(WO_4)_2$		5.3595	5.3595	11.6648	90
$NaLu(MoO_4)_2$		5.1592	5.1592	11.2422	90
$NaY(MoO_4)_2$		5.1975	5.1975	11.3412	90
$NaGd(MoO_4)_2$		5.2357	5.2357	11.4395	90
$NaLa(MoO_4)_2$		5.344	5.344	11.7373	90
$KLa(WO_4)_2$		5.445	5.445	12.1414	90
$KLa(MoO_4)_2$		5.397	5.397	12.1667	90
$KLu(WO_4)_2$	Monoclinic $C_{2/c}$ (15) [28]	10.5958	10.2387	7.5008	130.73
$KY(WO_4)_2$		10.6288	10.3417	7.5538	130.75
$KGd(WO_4)_2$		10.6844	10.4424	7.6038	130.8
$KLu(MoO_4)_2$	Orthorhombic P_{bcn}	5.3115	7.7719	18.3323	90
$KY(MoO_4)_2$	(60) [29]	5.0695	18.2080	7.9462	90
$KGd(MoO_4)_2$	Tridinic P_{-1} (2) [30]	11.1889	5.2844	6.9138	111.541

Table 2
Stokes Shift (cm^{-1}) of tetragonal compounds.

	$LiLn(WO_4)_2$	$NaLn(WO_4)_2$	$NaLn(MoO_4)_2$	$KLn(WO_4)_2$	$KLn(MoO_4)_2$
Lu		17570	15710		
Y		17820	16550		
Gd	18600	18510	16880		
La	19750	22270	16920	21456	17354